JURNAL KEDOKTERAN DIPONEGORO
(*DIPONEGORO MEDICAL JOURNAL*)
Online : http://ejournal3.undip.ac.id/index.php/medico
E-ISSN : 2540-8844
DOI : 10.14710/dmj.v14i5.49108
JKD (DMJ), Volume 14, Number 5, September 2025 : 233-242

PROPOSED MECHANISM OF ERLOTINIB-INDUCED RASH FORMATION IN RATS BASED ON THE SKIN EXPRESSION OF *CINC1* AND *TTP* mRNAs

Iqbal Julian[1]* Takuya Iwamoto[2]
[1] Department of Biomedical and Clinical Pharmacy, Faculty of Pharmacy, Universitas Pancasila, South Jakarta, Indonesia
[2] Department of Clinical Biopharmaceutics, Graduate School of Medicine, Mie University, Tsu, Japan

Keywords:
Erlotinib,
Mechanism,
Rash,
Tristetraprolin

Received: 9 January 2025
Revised: 2 June 2025
Accepted: 2 June 2025
Available online: 1 September 2025

Corresponding Author:
E-mail: miqbaljulian@univpancasila.ac.id

ABSTRACT

Background: Erlotinib's effect on the skin is greatly recognized to cause rashes. To treat the rashes effectively, it is necessary to understand the mechanism of rashes formation induced by the drug. However, the mechanism underlying the effect was not well-known. **Objective:** This study measured the *CINC1* and *TTP* mRNAs' expression to elaborate the mechanism. **Methods:** An experimental preclinical quantitative study was designed. Rats were divided into three groups: placebo, low dose, and high dose based on the involvement and dosage of erlotinib, and were treated for 7 days. The samples were collected from the blood on days 0 and 7 and the skin on day 7. The blood was used to measure the circulating concentration of CINC-1, whereas the skin was used to measure the tissue expression of *CINC1* and *TTP* mRNAs. **Results:** At mild rashes, the tissue expression of *CINC1* and *TTP* mRNAs tended to elevate compared to the placebo, while at severe rashes, the *TTP* mRNA was suppressed in contrast to the *CINC1* mRNA. The level of circulating CINC1 among the three groups following 7 days of treatment tended to elevate. **Conclusion:** The results suggest the involvement of CINC1 and TTP during the formation of erlotinib-induced rashes and the mechanism underlying the rashes formation was proposed accordingly. Furthermore, targeting these proteins could be a reference for a clinical study on the treatment of erlotinib-induced rashes.

BACKGROUND

Erlotinib is a tyrosine kinase inhibitor approved for the treatment of locally advanced or metastatic NSCLC (Non-Small Cell Lung Cancer). The inhibitor inhibits the EGFR (Epithelial Growth Factor Receptor) signaling pathway, resulting in reduced cancer cell proliferation, angiogenesis, and metastasis, and induced apoptosis.[1]

Erlotinib administration inflicts rashes as a common adverse event, occurring in 75% of the patients.[1] The severe rash can reduce the patients' QOL (Quality of Life). To improve the patient's QOL, in some cases, the erlotinib therapy is discontinued. Certainly, discontinued therapy will affect the clinical outcome of patients. Nevertheless, rashes severity correlates significantly with erlotinib effectiveness.[2] This means it is important to handle the skin rash without disrupting the erlotinib therapy to achieve the objective of the medication.

To be able to handle the skin rash, it is necessary to understand the mechanism of EGFR inhibitor-induced skin rash. Apoptosis due to the EGFR inhibition triggers inflammatory reactions in the skin.[3] One of the proinflammatory cytokines that are released during inflammatory reactions is CINC1. In humans, an elevated level of CINC1 (Chemokine-Induced Neutrophil Chemoattractant-1) is associated with dermatitis.[4] CINC1 is a peptide that promotes neutrophil migration to sites of inflammation.[5] It also enhances neutrophils' adhesion to fibrinogen and neutrophilic phagocytosis in a dose-dependent manner.[6]

JURNAL KEDOKTERAN DIPONEGORO
(*DIPONEGORO MEDICAL JOURNAL*)
Online : http://ejournal3.undip.ac.id/index.php/medico
E-ISSN : 2540-8844
DOI : 10.14710/dmj.v14i5.49108
JKD (DMJ), Volume 14, Number 5, September 2025 : 233-242

CINC1 mRNA contains AREs (AU-rich elements) in the 3' untranslated region (UTR).[7] Even so, AREs are found in *CINC1* mRNA and many mRNAs. AREs are a target of TTP (Tristetraprolin), a zinc finger protein that binds to AREs.[8] When TTP binds to AREs, it recruits factors that promote mRNA decay, leading to a decrease in protein levels.

Elaborating on the mechanism of erlotinib-induced rash in skin tissues, we focused on the observation of TTP and CINC1. From the above information, we thought that a mechanism similar to dermatitis also occurs in an erlotinib-induced rash. We hypothesized that the use of erlotinib would reduce the *CINC1* and *TTP* mRNAs expression in skin tissues and elevate the CINC1 expression in the circulation.

The investigation of *CINC1* and *TTP* mRNAs in this study is a novel approach to explain the mechanism of erlotinib-induced rashes. The TTP profile will clarify its role in the emersion of the rash and its correlation with CINC1 as a proinflammatory substance.

METHODS

Research Design

The mechanism of erlotinib-induced rashes was observed through the alteration of *CINC1* and *TTP* mRNAs expression in rats. The rats were divided into three groups: placebo, low dose, and high dose. The blood and skin from the rats were used as samples for analysis. The blood samples were used to measure the concentration of plasma biochemical parameters of hepatic and renal functions (Blood Urea Nitrogen, Creatinine, Aspartate Transaminase, Alanine Transaminase, and Total Bilirubin) and the erlotinib and CINC1 plasma concentrations. The skin samples were used to measure the expression of *CINC-1* and *TTP* mRNAs.

Tested Animals

This study used male, wild-type, 8–10-week-old Sprague Dawley rats. Food and water were placed on the roof of the cage and available for 24 hours.

Tested Solutions

The solvent was a saline-based solution where sodium carboxymethylcellulose 0.3% m/v and Tween 80 0.1% v/v were dissolved.[9] Erlotinib solutions were made as a single daily dose and given orally for seven days. The amount of erlotinib depended on the rat's BW (body weight). Therefore, it was measured before solution preparation. The measurement of body weight was done in the morning time. The placebo group received solely the solvent. The low-dose group received erlotinib 0.05 mg/g BW. The high-dose group received erlotinib 0.075 mg/g BW. The solvent was added to the weighed erlotinib to make 1.0–2.0 mL of the drug solution/100 g BW.[10] The solutions were administered to the rats after lunchtime.

Monitoring of Adverse Events

Adverse events were observed visually and recorded using a digital camera (Kodak EasyShare C182, China) each day. Sites of rash observation were the front legs, area around the skin and mouth, and back. A small area of hair on the back was shaved to get clear skin sightings. The body weight alteration was also observed.

Collection and Treatment of Blood Samples

Blood samples were collected through the orbital sinus just before the administration of the drug solution (day 0) and a day following the last day of drug administration (day 7) under anesthesia conditions.[11] The blood collection was conducted in the morning time. Around 1.0–1.5 mL of blood could be collected from each rat. The sample was kept in a heparinized 1.5 mL microtube and stored in a 4^{o}C ice box according to the World Health Organization's laboratory manual.[12] Soon after blood collection, the samples were centrifuged at 1700 x g for 10 minutes at 10^{o}C. The plasma samples were collected, kept in new tubes, and stored in a -30^{o}C refrigerator.

JURNAL KEDOKTERAN DIPONEGORO
(*DIPONEGORO MEDICAL JOURNAL*)
Online : http://ejournal3.undip.ac.id/index.php/medico
E-ISSN : 2540-8844
DOI : 10.14710/dmj.v14i5.49108
JKD (DMJ), Volume 14, Number 5, September 2025 : 233-242

Collection and Treatment of Skin Samples

Skin samples were collected through the rats' back on day 7 using a 2 mm skin biopsy punch.(13) The sample collection was done at 2 p.m. For each rat, two skin samples were collected. The two samples were used for measuring the *CINC1* and *TTP* mRNAs expression by using a qRT PCR. After the collection, the two samples were put in a 1.5 mL microtube and kept inside a 4ºC ice box.

Measurement of Plasma Concentration of Hepatic and Renal Function Biochemical Parameters

The plasma concentration of hepatic and renal function biochemical parameters was measured by FUJIFILM Wako Pure Chemical Industries, Osaka, Japan. Plasma BUN (blood urea nitrogen) level was measured based on the Urease-GIDH Method using L-Type UN reagent. Plasma CRE (creatinine) level was measured based on the Creatininase-HMMPS Method using L-Type Creatinine M reagent. Plasma AST (aspartate aminotransferase) and ALT (alanine aminotransferase) levels were measured based on the JSCC (Japan Society of Clinical Chemistry) Transferable Method using L-Type AST.J2 and L-Type ALT.J2 reagents, respectively. Whereas, plasma T-Bil (total bilirubin) level was measured based on the vanadate oxidation method using Total Bilirubin E-HA reagent.

Measurement of Erlotinib Plasma Concentration

Two hundred µL of plasma sample was mixed with 10 µL of 1 µg/mL of Erlotinib-d6 (Cosmo Bio Co. Ltd., Tokyo, Japan) as the internal standard. The sample was then mixed with 570 µL of methanol, vortexed, and centrifuged at 10,000 rpm for 10 minutes. The supernatant fluid was filtered with a 0.45-micron filter for chromatographic analysis.[14]

The concentrations of plasma erlotinib were measured by using LC-MS/MS. Agilent 1260 Infinity (Agilent Technologies, Tokyo) liquid chromatography (LC) system equipped with Zorbax Eclipse plus C18 2.1 x 100 mm 1.8-Micron (Agilent Technologies) was used and eluted using a gradient. The mobile phases were comprised of 5 mM ammonium acetate in distilled water and acetonitrile. Following the sample injection (2 µL), elution was performed by generating a gradient from 10 to 50% of acetonitrile in the initial 3 minutes, followed by a gradient from 50 to 90 of acetonitrile from 3 to 6 min. The total run time was 10 minutes per run and the flow rate was maintained at 0.35 mL/min at 40ºC. The retention time was 4.6 minutes for Erlotinib and Erlotinib-d6.[14]

The LC system was coupled with triple quadrupole MS/MS, Agilent 6490 (Agilent Technologies). The MS/MS was equipped with an electrospray ionization (ESI) source, operated in the positive ion mode, and the quantification was performed in the multiple reaction monitoring (MRM) mode with mass-to-charge (m/z) transition at 394.4 > 278.1 for Erlotinib and 400.2 > 278.1 for Erlotinib-d6. Nitrogen gas was used for nebulization, desolvation, and collision. The instrument conditions were set as follows: collision energy 28 V for Erlotinib and 32 V for Erlotinib-d6, capillary voltage 4.0 kV, dwell time 200 ms, sheath gas flow 12 L/min at 300ºC, desolvation gas flow 14 L/min at 250ºC, and 50 psi nebulization gas pressure. The data were acquired and analyzed using MassHunter Workstation software (Agilent Technologies). The ratios of the peak area of Erlotinib to that of Erlotinib-d6 were used for all calculations.[14]

The samples used for calibration were prepared by mixing Erlotinib stock solution with drug-free plasma, L-Consera (Nissui Pharmaceutical Co., Ltd, Tokyo). Seven different concentrations of calibration solutions were prepared to obtain a 7-point standard curve (1000, 500, 100, 50, 10, 5, 1 ng/mL).[14]

Measurement of Tissue *CINC1* and *TTP* mRNAs Expression

Two steps were taken before the skin samples were ready to be measured by qRT-PCR (quantitative Real-Time Poly Chain Reaction) system. The first step is the extraction of total RNA from the skin sample. The second step is the synthesis of cDNA from the total RNA.

Total RNA was prepared from fresh or frozen rat skin tissue using Fastpure™ RNA kit according to the manufacturer's protocol (Takara Bio Inc., Shiga), and the concentration was measured using NanoDrop 2000 Spectrophotometer (Thermo Fisher Scientific Inc., Wilmington, USA). To homogenize the skin sample, lysis buffer was added into the skin tissue-contained microtube, then homogenized using VP-5S UltraSonic Homogenizer supplied by Taitec at tune number 6 for 5 minutes.

JURNAL KEDOKTERAN DIPONEGORO
(*DIPONEGORO MEDICAL JOURNAL*)
Online : http://ejournal3.undip.ac.id/index.php/medico
E-ISSN : 2540-8844
DOI : 10.14710/dmj.v14i5.49108
JKD (DMJ), Volume 14, Number 5, September 2025 : 233-242

The synthesis of cDNA was done using a total RNA sample by ReverTra Ace® qPCR RT Master Mix with gDNA Remover kit according to the manufacturer's protocol (Toyobo Co., Ltd., Osaka). Then, the cDNA sample was processed using the EagleTaq Master Mix kit according to the manufacturer's protocol (Roche Diagnostics GmbH) before being measured by the qRT PCR system. GAPDH (glyceraldehyde 3-phosphate dehydrogenase) gene was chosen as the housekeeping gene. The GAPDH cDNA was amplified with the following oligonucleotides: forward primer 5'-TGGGAAGCTGGTCATCAAC-3'; reverse primer 5'-GCATCACCCCATTTGATGTT-3'. The CINC1 cDNA was amplified with the following oligonucleotides: forward primer 5'-CACACTCCAACAGAGCACCA-3'; reverse primer 5'- TGACAGCGCAGCTCATTG-3'. The TTP cDNA was amplified with the following oligonucleotides: forward primer 5'-GACTTCTGCGAACCGACTGT-3'; reverse primer 5'- CATGGCTCATCGACATAAGG-3'.

Later, the expression level of skin *CINC1* and *TTP* mRNAs was measured from the treated cDNA sample by StepOnePlus Real-Time PCR system using the operator's manual of the thermal cycler supplier (Applied Biosystems, California, USA). The qRT-PCR was run using the following method: holding stage, step 1 at 50.0 ºC for 2 minutes, step 2 at 95.0 ºC for 10 minutes; cycling stage, step 1 at 95.0 ºC for 15 seconds, step 2 at 60.0 ºC for 1 minute, the starting cycle was 1, the number of cycles was 60 cycles.

Measurement of CINC1 Plasma Concentration

The CINC1 plasma concentration was measured using Quantikine® ELISA Rat CXCL1/CINC-1 Immunoassay (R&D Systems®, Minneapolis, USA). The procedure was done according to the package insert.

Statistical Analyses

This study used GraphPad Prism® 5 version 5.01 for Windows to perform statistical analyses. Kruskal-Wallis's test was conducted to determine differences between three groups on body weight changes; plasma concentrations of hepatic and renal function biochemical parameters at day 0 and day 7; RQ (Relative Quantification) value of *TTP* and *CINC1* mRNAs; and changes in plasma CINC1 concentrations. Dunn's multiple comparison tests were performed as a post-test of the Kruskal-Wallis's test.

RESULTS

Physical Observation

The rat's physical changes were observed through the alteration of body weight and rash appearance. On day 0, which was soon before treatments, the physical quality among rats in each group was similar to each other.

On day 7, the body weight alteration was observed among the groups. The reduction was observed in low and high dose groups, whereas elevation was seen in the placebo group as shown in Fig. 1. The body weight reduction is suggested due to anorexia and diarrhea.

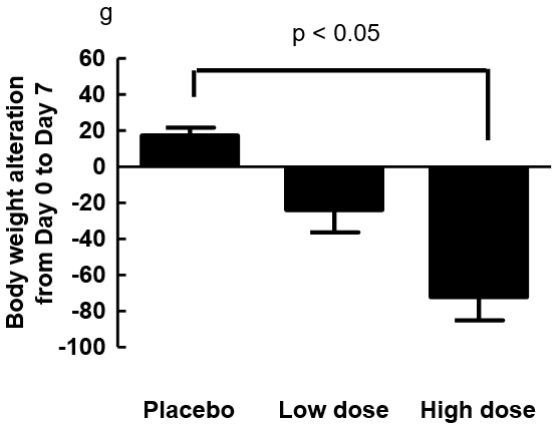

Figure 1. Body Weight Alteration among the Groups (n = 4) from day 0 to day 7

JURNAL KEDOKTERAN DIPONEGORO
(*DIPONEGORO MEDICAL JOURNAL*)
Online : http://ejournal3.undip.ac.id/index.php/medico
E-ISSN : 2540-8844
DOI : 10.14710/dmj.v14i5.49108
JKD (DMJ), Volume 14, Number 5, September 2025 : 233-242

The rash appeared in low and high-dose groups on day 7. The rash in the high-dose group was relatively more severe than in the low-dose group as shown in Fig. 2. The placebo group had not experienced rash.

(a)

(b)

(c)

Figure 2. Rash Comparison among the Groups on Day 7: (a) Placebo, (b) Low Dose, and (c) High Dose

Plasma Concentration of Hepatic and Renal Function Biochemical Parameters

Creatinine, alanine transaminase, and total bilirubin plasma concentrations tended to elevate in erlotinib-treated groups as compared to the placebo group, as shown in Table 1. These indicated interfered-renal and hepatic functions in erlotinib-treated groups.

JURNAL KEDOKTERAN DIPONEGORO
(*DIPONEGORO MEDICAL JOURNAL*)
Online : http://ejournal3.undip.ac.id/index.php/medico
E-ISSN : 2540-8844
DOI : 10.14710/dmj.v14i5.49108
JKD (DMJ), Volume 14, Number 5, September 2025 : 233-242

Table 1. Plasma Concentration of Hepatic and Renal Function Biochemical Parameters

		Placebo (n = 3)	Low dose (n = 3)	High dose (n = 3)
BUN (mg/dL)	Day 0	12.9 ± 1.05	12.2 ± 1.19	14.7 ± 0.80
	Day 7	12.8 ± 1.62	13.6 ± 0.36	60.0 ± 49.5
CRE (mg/dL)	Day 0	0.27 ± 0.02	0.28 ± 0.01	0.30 ± 0.01
	Day 7	0.29 ± 0.01*	0.33 ± 0.02*	0.90 ± 0.64
AST (IU/L)	Day 0	62.0 ± 4.90	67.3 ± 10.1	73.3 ± 17.3
	Day 7	73.3 ± 26.6	61.3 ± 7.59	121 ± 58.3
ALT (IU/L)	Day 0	33.7 ± 1.89	37.7 ± 1.70	48.7 ± 10.6
	Day 7	34 ± 0*	38.3 ± 2.87*	47.7 ± 13.7
T-Bil (µg/dL)	Day 0	20.0 ± 8.17	16.7 ± 4.71	30.0 ± 8.17
	Day 7	23.3 ± 4.71*	240 ± 283	6340 ± 1220*

Kruskal-Wallis's test followed with Dunn's test, α = 0.05, * means p value among 2 groups < α

Erlotinib Plasma Concentration

The erlotinib plasma concentration among the groups is shown in Table 2. The difference in erlotinib plasma concentration between the high-dose group and placebo group was elevated multiple times than the difference between the low-dose group and placebo group. The enhanced erlotinib plasma concentration in the high-dose group was probably due to the interfered renal and hepatic functions.

Table 2. Erlotinib Plasma Concentration

	Placebo (n = 3) (µg/mL)	Low Dose (n = 3) (µg/mL)	High Dose (n = 3) (µg/mL)
Day 0	N.D.	N.D.	N.D.
Day 7	N.D.	1.72 ± 1.88	90.6 ± 35.3

N.D.: Not Detected, < 10.0 ng/mL Mean ± S.D.

Tissue Expression of *CINC1* and *TTP* mRNAs

The tissue expression of *CINC1* and *TTP* mRNAs among the groups on day 7 is shown in Fig. 3. Tissue expression of mRNAs was measured based on the RQ value obtained from the qRT-PCR analysis of rats' skin samples. The tissue expression of *CINC1* mRNA tended to elevate with the addition of erlotinib dosage, whereas the *TTP* mRNA did not.

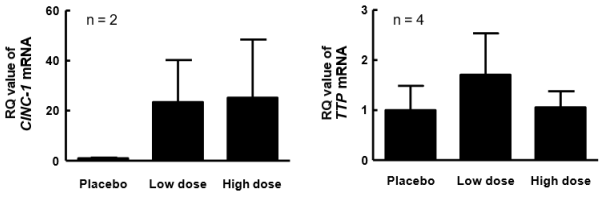

Figure 3. Tissue Expression of *CINC1* and *TTP* mRNAs on Day 7

CINC1 Plasma Concentration

The CINC1 plasma concentration among the groups on day 7 is shown in Fig. 4. The CINC1 plasma concentration tended to elevate with the addition of erlotinib dosage.

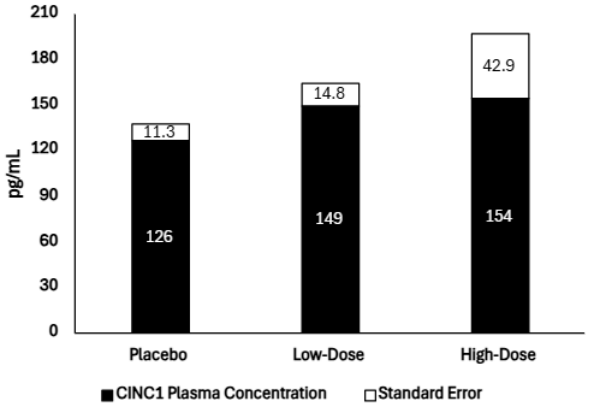

Figure 4. CINC1 Plasma Concentration on Day 7

JURNAL KEDOKTERAN DIPONEGORO
(*DIPONEGORO MEDICAL JOURNAL*)
Online : http://ejournal3.undip.ac.id/index.php/medico
E-ISSN : 2540-8844
DOI : 10.14710/dmj.v14i5.49108
JKD (DMJ), Volume 14, Number 5, September 2025 : 233-242

DISCUSSIONS

Rashes are the most common adverse event of erlotinib. However, the underlying rash mechanism is not fully understood. This study was conducted, driven by the understanding of the mechanism would benefit the handling of erlotinib-induced rashes. In humans, an elevated level of CINC1 is associated with dermatitis. *CINC1* mRNA contains AREs in the 3' untranslated region and these AREs are a target of TTP. We proposed this preclinical study to explain the mechanism of erlotinib-induced rash based on tissue expression of *CINC1* and *TTP* mRNAs.

This study was conducted using wild male Sprague-Dawley rats to meet the objective of the research. The dosages of erlotinib in this study were established to cause rashes within 7 days of drug administration. However, the lower dosage of erlotinib used in this study was still higher as compared to the erlotinib dosage for clinical use. By examining hepatic and renal function, the appropriateness of the dosages in this study could be used as a reference for clinical use. Both low-dose and high-dose groups experienced adverse events within seven days. Anorexia, rash, and diarrhea are the adverse events that could be detected in this study. Anorexia and diarrhea could be interpreted as the incidence of the loss of body weight.[15,16] These adverse events are like humans.

From the measurement of plasma concentration of hepatic and renal function biochemical parameters, the total bilirubin concentration in the high-dose group was elevated significantly as compared to the placebo group following 7 days of drug administration. Elevated total bilirubin plasma concentration indicates liver injury that declines the hepatic function.

The liver injury would affect the metabolism and elimination of erlotinib. Erlotinib metabolism is mediated predominantly in the liver and intestine,[17] and its elimination occur through the feces (83%) and urine (8%).[18] The disruption in metabolism and elimination would extend the presence of erlotinib in circulation and intensively distribute it to the tissues. It caused the adverse events to be more severe in high-dose groups. The injured liver caused erlotinib plasma concentration in the high-dose group to elevate multiple times as compared to the low-dose group.

Skin sample analysis using qRT-PCR was conducted to observe the expression level of *CINC1* and *TTP* mRNAs. Even though the total RNA concentrations were small, the result of qRT-PCR could still be obtained. To deal with small total RNA concentrations, further sample preparation was modified. The cDNA synthesizing procedure was modified by substituting nuclease-free water with the total RNA sample to get the expected results. The modified procedure also appeared in the sample preparation for cDNA target detection by substituting distilled water with the cDNA sample.

Of the PCR results, the *CINC1* mRNA tissue expression of the low-dose group tended to have higher levels as compared to the placebo following 7 days of treatment. The trend seems to depend on erlotinib plasma concentration and, thus, the degree of inflammation. Indeed, the highest *CINC1* mRNA tissue expression was observed in the high-dose group. In the erlotinib-treated groups, the inflammatory reaction occurred, thus the *CINC1* mRNA tissue expression was elevated as well as the CINC1 plasma concentration.

On the other hand, the *TTP* mRNA tissue expression seems not to depend on the erlotinib plasma concentration but on the degree of inflammation. In a mild-moderate inflammation, as represented in the low-dose group, the *TTP* mRNA tissue expression was aligned with the elevated tissue expression of *CINC1* mRNA. The elevated *TTP* mRNA tissue expression is taught as the negative feedback mechanism to control the inflammatory reaction. However, in severe inflammatory conditions, as represented in the high-dose group, the *TTP* mRNA tissue expression seems to be suppressed to accommodate enhanced inflammatory reaction due to a severe tissue injury. The suppressed *TTP* mRNA tissue expression could explain the further elevation

JURNAL KEDOKTERAN DIPONEGORO
(*DIPONEGORO MEDICAL JOURNAL*)
Online : http://ejournal3.undip.ac.id/index.php/medico
E-ISSN : 2540-8844
DOI : 10.14710/dmj.v14i5.49108
JKD (DMJ), Volume 14, Number 5, September 2025 : 233-242

of *CINC1* mRNA tissue expression and CINC1 plasma concentration.

TTP has two forms that are characterized by its stability and activeness: phosphorylated and dephosphorylated forms. Phosphorylated TTP is structurally stable but inactive, while the dephosphorylated one is structurally unstable but active. When inflammation occurs, phosphorylated TTP is abundant, thus the *CINC1* mRNA tissue expression is elevated. It explained the elevation of *CINC1* mRNA tissue expression in the low-dose group. Conversely, when the inflammation is resolved, dephosphorylated TTP is abundant, thus the *CINC1* mRNA expression is declined and further the CINC1 plasma concentration. Dephosphorylation of TTP is activated by PP2A (Protein Phosphatase 2A).[19]

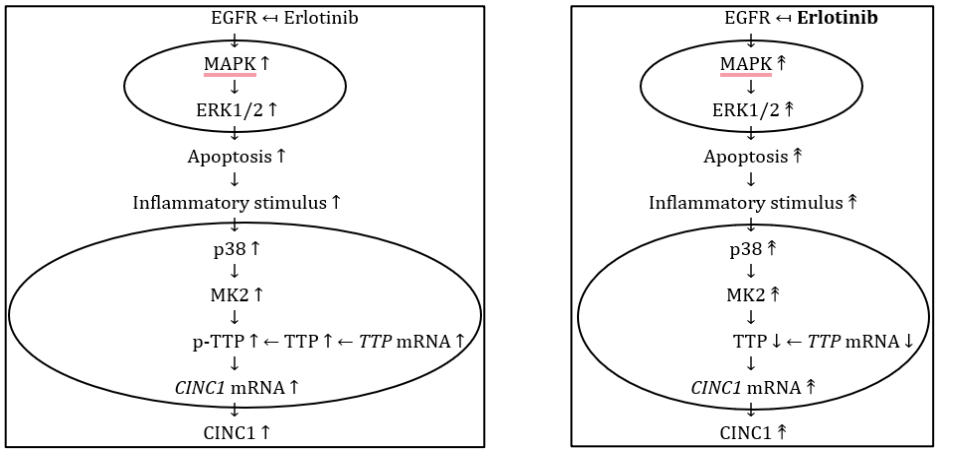

Annotation:
Erlotinib (with bold word): high dose
Erlotinib (without bold word): low dose
↑: elevated activation or synthesis
↟: enhanced elevated activation
↓ (following *TTP* mRNA): reduced synthesis
↓: consequence
↤: inhibited activation

Figure 5. A Proposed Molecular Mechanism of EGFR Inactivation in Erlotinib-Induced Rashes in Rats in Mild-Moderate (left) and Severe (right) Inflammatory Reactions

As shown in Fig. 5, the inhibition of the EGFR signaling pathway leads to the inactivation of the ERK1/2 signaling pathway.[20] The inactivation of the ERK1/2 signaling pathway leads to apoptosis.[21] Excessive apoptosis triggers the inflammatory stimulus. The inflammatory stimulus caused by the cell death activates the p38 signaling pathway in the neighbor cells.[22] It also elevates the TTP expression. The activation of p38 also activates the MK2,[23] which further phosphorylates the TTP.[24] The phosphorylated TTP is inactive. The inactive TTP causes the stabilization of lots of proinflammatory mRNA such as *CINC1* mRNA, thus elevating its expression (Fig. 3). Elevated *CINC1* mRNA causes the elevation of circulating CINC1 expression (Fig. 4). At a higher dose, the erlotinib-induced skin damage was more severe (Fig. 2) and the inflammatory stimulus was stronger. A stronger inflammatory stimulus is likely to suppress the *TTP* mRNA synthesis (Fig. 3).[25] This causes a relatively higher CINC1 secretion (Fig. 4) and, thus, more severe inflammatory reactions.

The data generated in this study will form a foundation for the clinical study of EGFR inhibitor-induced skin toxicity. The provided mechanism could be used as a reference to target molecules for diagnostic biomarkers, drug development, and therapeutic management studies on erlotinib-induced rashes. However, the number of samples in this study is relatively small. More samples would be needed to validate our results.

CONCLUSIONS

From this preclinical study, in mild to moderate rashes, erlotinib tends to elevate the synthesis of *CINC1* and *TTP* mRNAs and elevate the secretion of circulating CINC1. However, in severe rashes, the synthesis of *TTP* mRNA is likely to be suppressed. This suppression causes further elevation of CINC1 expression. The mechanism of erlotinib-induced

rashes is proposed according to the literature study and interpretation of the results above.

ETHICAL APPROVAL

The Health Research Ethics Committee, Graduate School of Medicine, Mie University, ethically approved this study based on the Ethical Approval no. 20-10 R3 for in vivo Pharmacokinetic Study.

CONFLICT OF INTEREST

Competing interests: No relevant disclosures.

FUNDING

A grant from the Ministry of Education, Culture, Sports, Science and Technology of Japan for international graduate students supported this study.

AUTHORS CONTRIBUTION

Study conception and design: IJ, TI; data collection: IJ, TI; analysis and interpretation of results: IJ; draft manuscript preparation: IJ. All authors reviewed the results and approved the final version of the manuscript.

ACKNOWLEDGMENTS

Our acknowledgement to the Ministry of Education, Culture, Sports, Science and Technology of Japan for supporting this study.

REFERENCES

1. Abdelgalil AA, Al-Kahtani HM, Al-Jenoobi FI. Chapter Four - Erlotinib. In: Brittain HG, editor. Profiles of Drug Substances, Excipients, and Related Methodology [Internet]. Academic Press; 2020. p. 93–117. (Profiles of Drug Substances, Excipients and Related Methodology; vol. 45). Available from: https://www.sciencedirect.com/science/article/pii/S1871512519300196
2. Komiya N, Takahashi K, Kato G, Kubota M, Tashiro H, Nakashima C, et al. Acute Generalized Exanthematous Pustulosis Caused by Erlotinib in a Patient with Lung Cancer. Case Rep Oncol. 2021 Jan 1;14(1):599–603.
3. Eissa IH, G.Yousef R, Elkady H, Elkaeed EB, Alsfouk AA, Husein DZ, et al. A new anticancer derivative of the natural alkaloid, theobromine, as an EGFR inhibitor and apoptosis inducer. Theor Chem Acc [Internet]. 2023;143(1):1. Available from: https://doi.org/10.1007/s00214-023-03071-z
4. Xiao T, Sun M, Kang J, Zhao C. Transient Receptor Potential Vanilloid1 (TRPV1) Channel Opens Sesame of T Cell Responses and T Cell-Mediated Inflammatory Diseases. Vol. 13, Frontiers in Immunology. Frontiers Media S.A.; 2022.
5. Tomonaga T, Higashi H, Izumi H, Nishida C, Kawai N, Sato K, et al. Investigation of pulmonary inflammatory responses following intratracheal instillation of and inhalation exposure to polypropylene microplastics. Part Fibre Toxicol [Internet]. 2024;21(1):29. Available from: https://doi.org/10.1186/s12989-024-00592-8
6. Xing D, Hage FG, Feng W, Guo Y, Oparil S, Sanders PW. Endothelial cells overexpressing CXCR1/2 are renoprotective in rats with acute kidney injury. Am J Physiol Renal Physiol. 2023 Apr 1;324(4):F374–86.
7. Barreau C, Paillard L, Osborne HB. AU-rich elements and associated factors: are there unifying principles? Nucleic Acids Res [Internet]. 2005 Dec 1;33(22):7138–50. Available from: https://doi.org/10.1093/nar/gki1012
8. Hsieh HH, Chen YA, Chang YJ, Wang HH, Yu YH, Lin SW, et al. The functional characterization of phosphorylation of tristetraprolin at C-terminal NOT1-binding domain. J Inflamm [Internet]. 2021;18(1):22. Available from: https://doi.org/10.1186/s12950-021-00288-2
9. Abraham J, Nelon LD, Kubicek CB, Kilcoyne A, Hampton ST, Zarzabal LA, et al. Preclinical Testing of Erlotinib in a Transgenic Alveolar Rhabdomyosarcoma Mouse Model. Sarcoma [Internet]. 2011;2011(1):130484. Available from: https://onlinelibrary.wiley.com/doi/abs/10.1155/2011/130484
10. Krinke G. The Laboratory Lab. 1st ed. Bullock G, Bunton T, editors. Academic Press; 2000. 463–482 p.
11. S P, R R, R K. Blood sample collection in small laboratory animals. J Pharmacol Pharmacother

[Internet]. 2010;1(2):87–93. Available from: https://doi.org/10.4103/0976-500X.72350
12. Blacksell S, Hughes T, Lee M, Lee J. A guide for the practical implementation of the WHO laboratory biosafety manual [Internet]. 4th ed. World Health Organization; 2023. Available from: http://apps.who.int/bookorders.
13. Nischal U, KC N, Khopkar U. Techniques of Skin Biopsy and Practical Considerations. 1. Available from: https://doi.org/10.4103/0974-2077.44174
14. Julian I, Iwamoto T. Investigation of Biomarkers and Handling Strategy of Erlotinib-Induced Skin Rash in Rats. Biol Pharm Bull. 2021;44(8):1050–9.
15. Schöttle J, Chatterjee S, Volz C, Siobal M, Florin A, Rokitta D, et al. Intermittent high-dose treatment with erlotinib enhances therapeutic efficacy in EGFR-mutant lung cancer [Internet]. Vol. 6, Oncotarget. 2015. Available from: www.impactjournals.com/oncotarget /
16. Zang YS, Fang Z, Li B. Erlotinib Plus Parenteral Nutrition: An Opportunity to Get Through the Hardest Days of Advanced Non-Small Cell Lung Cancer With Cancer Anorexia–Cachexia Syndrome. American Journal of Hospice and Palliative Medicine® [Internet]. 2013;30(2):210–3. Available from: https://doi.org/10.1177/1049909113476930
17. Zayed A, Al Hroot J, Mayyas A, Al-Husein B. Rapid high performance liquid chromatography method for erlotinib quantification in vitro: Application to study the effect of resveratrol on metabolism and cellular uptake of erlotinib. Fundam Clin Pharmacol [Internet]. 2023;37(5):983–93. Available from: https://onlinelibrary.wiley.com/doi/abs/10.1111/fcp.12914
18. Carter J, Tadi P. StatPearls [Internet]. 2024 [cited 2025 Jan 9]. Erlotinib. Available from: https://www.ncbi.nlm.nih.gov/books/NBK554484/
19. Rappl P, Brüne B, Schmid T. Role of Tristetraprolin in the Resolution of Inflammation. Biology (Basel) [Internet]. 2021;10(1). Available from: https://www.mdpi.com/2079-7737/10/1/66
20. Wei SG, Yu Y, Felder RB. TNF-α-induced sympathetic excitation requires EGFR and ERK1/2 signaling in cardiovascular regulatory regions of the forebrain. American Journal of Physiology-Heart and Circulatory Physiology [Internet]. 2021;320(2):H772–86. Available from: https://doi.org/10.1152/ajpheart.00606.2020
21. Sipieter F, Cappe B, Leray A, De Schutter E, Bridelance J, Hulpiau P, et al. Characteristic ERK1/2 signaling dynamics distinguishes necroptosis from apoptosis. iScience [Internet]. 2021 Sep 24;24(9). Available from: https://doi.org/10.1016/j.isci.2021.103074
22. Canovas B, Nebreda AR. Diversity and versatility of p38 kinase signalling in health and disease. Nat Rev Mol Cell Biol [Internet]. 2021;22(5):346–66. Available from: https://doi.org/10.1038/s41580-020-00322-w
23. Beamer E, Corrêa SAL. The p38MAPK-MK2 Signaling Axis as a Critical Link Between Inflammation and Synaptic Transmission. Vol. 9, Frontiers in Cell and Developmental Biology. Frontiers Media S.A.; 2021.
24. Rezcallah MC, Al-mazi T, Ammit AJ. Cataloguing the phosphorylation sites of tristetraprolin (TTP): Functional implications for inflammatory diseases. Cell Signal [Internet]. 2021;78:109868. Available from: https://www.sciencedirect.com/science/article/pii/S0898656820303454
25. Jiang W, Zhu D, Wang C, Zhu Y. Tumor suppressing effects of tristetraprolin and its small double-stranded RNAs in bladder cancer. Cancer Med [Internet]. 2021;10(1):269–85. Available from: https://onlinelibrary.wiley.com/doi/abs/10.1002/cam4.3622